Structural and electrical properties of Mg-doped vanadium dioxide thin films via room-temperature ion implantation

B.M. Mabakachaba[a,c,*], I.G. Madiba[b,c], J. Kennedy[e], K. Kaviyarasu[b,c], P. Ngoupe[d], B.S. Khanyile[b,c], J.J. Van Rensburg[d], F. Ezema[b], C.J. Arendse[a], M. Maaza[b,c]

[a]Department of Physics, University of the Western Cape, Robert Sobukwe Rd, Bellville, Cape town 7535, South Africa
[b]UNESCO-UNISA Africa Chair in Nanosciences/Nanotechnology, College of Graduate Studies, University of South Africa (UNISA), Muckleneuk Ridge, P O Box 392, Pretoria, South Africa
[c]iThemba LABS-National Research Foundation, 1 Old Faure Road, Somerset West 7129, PO Box 722, Somerset West, Western, Cape Province, South Africa
[d]Physics Department, University of Pretoria, Lynnwood Rd, Hatfield, Pretoria 0002, South Africa
[e]National Isotope Centre, GNS Science, PO Box 31312, Lower Hutt, New Zealand

*Correspondence to: mabakachaba@gmail.com

Highlights

- Successful deposition of (011) preferential phase monoclinic structure of VO_2 thin films by PLD.
- Mg ion implantation at higher fluence above 1×10^{17} ions/cm^2 result in the degradation of the defined VO_2 structure.
- At higher fluence MgO phase is prevalent at the surface of VO_2 resulting in the loss of thermochromism.
- Mg content tend to increase the carrier concentration, whilst increasing the work function parameter due to the displacement damage and defects induced.
- •Dose implants affect the abrupt nature of VO_2 SMT and stabilizing the monoclinic phase as the temperature increases.

Abstract

We report on the structural and electrical properties of Mg ion implanted semiconductor-metal transition of vanadium dioxide thin films with three different ion fluences. The effect of introducing Mg implants showed interchange, rearrangement, and modification of atoms in the lattice structure of VO_2. The (011) monoclinic signature of VO_2 is significantly affected; (i) peak broadening and shift of the peak position to lower angles at 1×10^{15} ions/cm^2, (ii) revert and shift towards high angles at 1×10^{16} ions/cm^2 and (iii) ceasing to exist at 1×10^{17} ions/cm^2 suggesting a complete devolution of the VO_2 thin films at higher fluence. Composition and profiling of the V-O matrix revealed a corresponding decrease of the vanadium edge peak at 1×10^{17} ions/cm^2 and a decrease of the oxygen content in implanted films. Whilst the carrier concentration is increased, the magnitude of the semiconductor-metal transition of implanted VO_2 thin films is significantly affected with a decrease of career mobility. Whilst increasing ion fluence above 1×10^{17} ions/cm^2 at a depth of 40 nm, the Mg implants move relatively towards the surface of VO_2 resulting in the loss of the characteristic thermochromism of VO_2 films.

Keywords: Mg-implatedVanadium dioxide; Ion implantation; Fluence; Transition phase; Electrical properties; Thin flim; SIMNRA; Rutherford backscattering spectroscopy (RBS)

1. Introduction

Materials with first-order phase transition are well studied and have attracted a great of attention in optoelectronic applications. One of the most fascinating oxides among others is vanadium dioxide (VO_2) due to its ultrafast reversible phase transition (monoclinic semiconductor – rutile metal phase) at temperature relatively close to room temperature (T_{tr}=68 °C) [1], [2], [3], [4]. The temperature-driven phase transition is also associated with a rapid resistivity change and this characteristic made VO_2 a potential material for resistive switching devices [5,6]. However, the material has major drawbacks which hinder real applications, such as high transition temperature (T_{tr}), low luminous transparency (T_{lum}) at temperatures above T_{tr}, wide hysteresis width, the unfavourable brown-yellowish colour of the film and lastly the alteration of the film's properties with time since it is not thermodynamically stable oxide [5,7].

In order to overcome these drawbacks, proposed mechanisms such as deposition methods, modification, design, and understanding of the physics behind the ultrafast phase transition of VO_2, have advanced for the development of potential applications. Maaza et. al, reported on the successfully synthesized pulsed laser VO_2 nano-coatings as optical limiters for Nd-Yag sources [8]. Further reports emerged demonstrating the possibility to engineer reversible and tunable VO_2 nano-scaled thin films by pulsed laser deposition (PLD) for potential femtosecond tunable optoelectronic nano-gating [9]. High quality monoclinic rutile-type vanadium dioxide (VO_2) (M1) nano-particles were synthesized by PLD without post-annealing and on a glass substrate. The films demonstrated a reversible metal-to-insulator transition at ~43 °C, without any doping, paving the way to switchable transparency in optical materials at room temperature [10]. Introducing dopants has proven to be the most effective way to alter and modify the characteristic properties of pure VO_2 thin films.

Previous studies have exceedingly reported on the modification of the semiconductor-metal transition properties of VO_2 using dopants such as Tin (Sn)[11], Aluminium (Al) [12,13], Tungsten (W) [13,17,[20], [21], [22], [23]], Molybdenum (Mo) [16,24], Niobium (Nb) [25], Magnesium (Mg) [26, 27], Titanium (Ti) [16,19], Fluorine (F) [15,20], Silicon (Si) [18] and Cesium (Ce0 [14]. Overall conclusions that Tungsten (W) is the most effective dopant for reducing the transition temperature (T_{tr}) much closer to room temperature [27], [28], [29] whilst Mg has also been well reported to effectively reduce T_{tr} and further increase the transmission properties of VO_2 (T_{lum}) [27, 30]. Most of these reports used solution-based and chemical methods such as spin-coating and hydrothermal synthesis for doping of VO_2 films. Bulk and surface property modification of VO_2 thin films are significant for a wide range of optoelectronic applications.

In this study; we use standard microelectronics technique of ion implantion to dope the VO_2 thin films. Ion implantation is particularly of interest in this work since it has better advantages compared to diffusion methods. Dopants can be introduced in a semiconductor in a more controlled way as compared to chemical doping techniques and can be easily repeated [31,32]. Synthesis of the VO_2 (M)/VO_2 (R) requires a controlled process that provides the necessary oxygen stoichiometry and correct crystalline structure because vanadium has different many oxidation states such as V_2O_5, V_2O_3, and VO. In this study, pristine VO_2 thin film was deposited by the PVD 3000 fully automated laser ablation system. Compared with other conventional laser ablation deposition and physical deposition methods, the PVD 3000 scanning options make it possible to obtain a very good homogeneity and uniformity of thin metallic layers on surfaces with very good control on the deposition temperature [33].

Magnesium was chosen as the doping material via ion beam implantation technology without conducting any post-treatment for the recrystallization of the implanted film, recovery and improvement of thermochromism. Nanothermochromics of Mg-doped VO_2 Mg has been reported to effectively reduce T_{tr} of VO_2 and additional benefits for practical arrangement and design of smart window technology such as a less yellowish appearance [27]. Panagopoulou et.al reported on the thermochromic performance of Mg-doped VO_2 thin films on functional substrates for glazing applications. They recorded the lowest transition temperature for Mg-doped VO_2 at T_{tr} = 35 °C using reactive magnetron sputtering on deposited on glass coated with SnO_2 buffer layer and, ZnO/glass substrates [34]. The effect of modification and property change of Mg-doped VO_2 thin films studied by XRD, RBS, Hall-Effect and Four-point probe measurements.

2. Experimental details: synthesis and ion implantation of VO_2

100 nm thick VO_2 thin film deposited on a diameter Si (100) substrate was used in the study and these samples were fabricated by reactive pulsed laser deposition (RDLP) technique, equipped with KrF laser wavelength of 248 nm and a vacuum base pressure of 10^{-6} Torr. The target (vanadium)-substrate distance was set at around 6.5 cm for a good uniformity of the thickness film, with substrate temperature kept at 500 °C in a pure oxygen environment. 1 × 1 cm deposited thin films of VO_2 were implanted with 35 KeV Mg ions at room temperature using the GNS ion implanter [35] for three different fluences (1×10^{15}, 1×10^{16} and 1×10^{17} ion cm^{-2}) as schematically shown in Fig. 1.

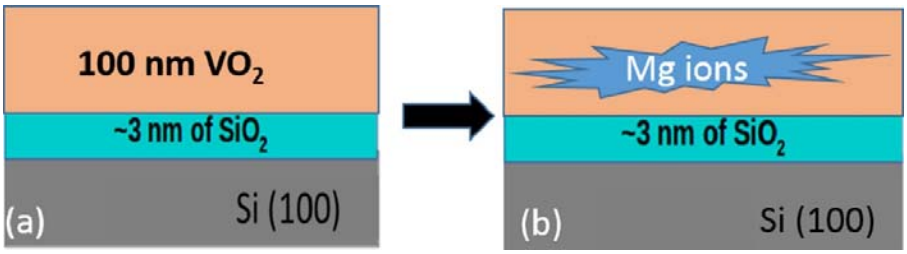

Fig. 1. Schematic representation of (a) pristine VO_2 film and (b) implanted VO_2 thin film.

Grazing incident x-ray diffraction (GIXRD) using a Cu-Kα (λ= 1.5406Å) radiation source was used for structural characterization of pristine VO_2 film and Mg-doped VO_2. Si substrates have intense crystalline peaks as well in the same region you would expect the VO peaks, thus it would make the diffractogram interpretation difficult. Grazing incidence XRD (GIXRD) geometry have been used to analyze the VO_2 on Si (100) have been used to overcome such limitations of the conventional XRD, to render the XRD measurement more sensitive to the near-surface region of the sample and minimize the substrate contribution on the diffraction response. The stoichiometry and thickness were characterized using Rutherford backscattering (RBS) with $4He^+$ ions of 2 MeV energy. Hall-effect measurements were carried out using the Ecopia HMS-300 hall measurement system to evaluate the carrier concentration, mobility, and resistivity of the samples. The measurements were conducted at room temperature using 0.55 Tesla permanent magnet in the four-probe configuration. In a four-wire resistivity measurements, the current is passed through the film through two leads, and the other two leads measure the potential difference across the sample.

3. Results and discussion

3.1. Structural analysis of VO_2: Mg

Prior to implantation, DYNAMIC-TRIM [36] simulations were performed to calculate Mg depth profiles for the 35 keV implantation with fluences between 1×10^{15} ions cm^{-2} and 1×10^{17} ions cm^{-2}. The profiles are shown in Fig. 2. The calculations predict a mean projected range of 40 nm coupled with a maximum implantation depth of around 80 nm. For these fluences, the Mg peak concentration varies between 0.2 and 17 at%. At fluences larger than 1×10^{16} Mg cm^{-2}, the Mg profile intersects with the surface. The peak broadening relative to the implant fluence also suggests the inhomogeneity of the Mg atomic states both at the surface and bulk proportion of VO_2 thin films. Furthermore, grazing incident XRD (GIXRD) measurements were performed to study the structural evolution; correspondence of the pristine and implanted VO_2 films with the known crystal orientations of vanadium oxides.

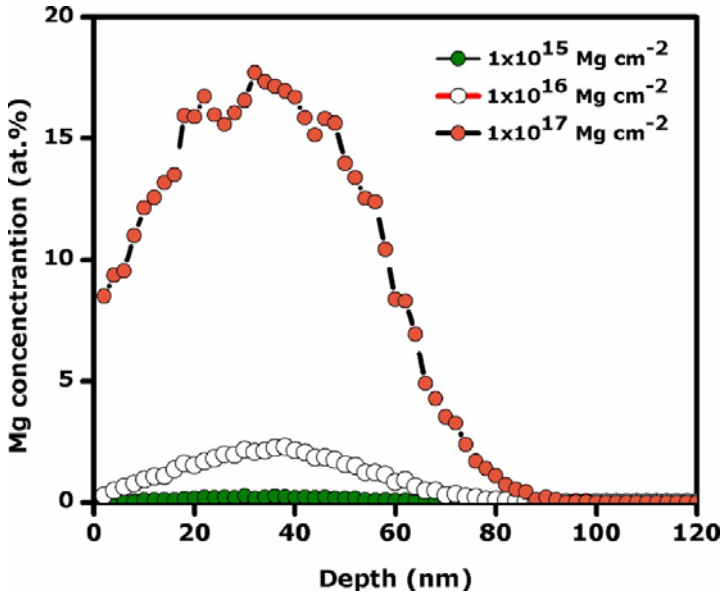

Fig. 2. Dynamic-TRIM of 35 KeV Mg simulated profile of Mg ions implanted in VO_2 film.

Fig. 3 illustrates the comparison of the GIXRD patterns of the pristine film with the implanted films at different fluences 1×10^{15}, 1×10^{16} and 1×10^{17} ions/cm^2.

The principle and geometry of the GIXRD is modified from a conventional XRD geometry to provide an "asymmetric" diffraction pattern, which allows access to small depths in the sample by varying the incidence angle (ω) between 1° and 3° for clear diffractograms analysis of the vanadium oxide films. The GIXRD pattern of the pristine film is a close match to the 00-043-1051 JCPDS pattern, the monoclinic structure corresponding to the space group P21/c with lattice parameters *a*=5.75170, *b*=4.53780 and *c*= 5.38250.

The GIXRD pattern of pristine and Mg-doped VO_2 thin films together with the reference diffractograms are illustrated in Fig. 3 while Fig. 4 illustrates the effect of Mg implantation on the dominant (011) orientation of the films where the peak position, width and the structural evolution of the films are evaluated by the Debye scherer approximation which is represented by the embbeded diagram. The analysis reveal that the pristine films are

polycrystalline in nature with monoclinic crystal structure. The (011), (211) and (022) orientation were observed for the pristine VO_2 film as demonstrated in the figure above with the preferred (011) phase at peak position of $2\theta = 28.33$ and a width of about $W_{h/2} = 0.4256$. Distinctive effects of the Mg ion on the crystal structure of VO_2 at different fluence are as follows: **(i)** Rearrangement of the (011) peak position. The implantation effect is inhomogeneous and ambiguously ascribed to a change in the defect configuration, occupying interstitial locations leading to the rearrangement of dissimilar atoms in the lattice structure [37,38]. After the Mg fluence of 1×10^{15} ion/cm^2, the VO_2 film maintained the preferred crystal orientation with a decrease of peak intensity and broadening ($W_{h/2} = 0.62017$) and a slight shift of the peak position (2θ ~27.9294) to lower phase angles was observed.

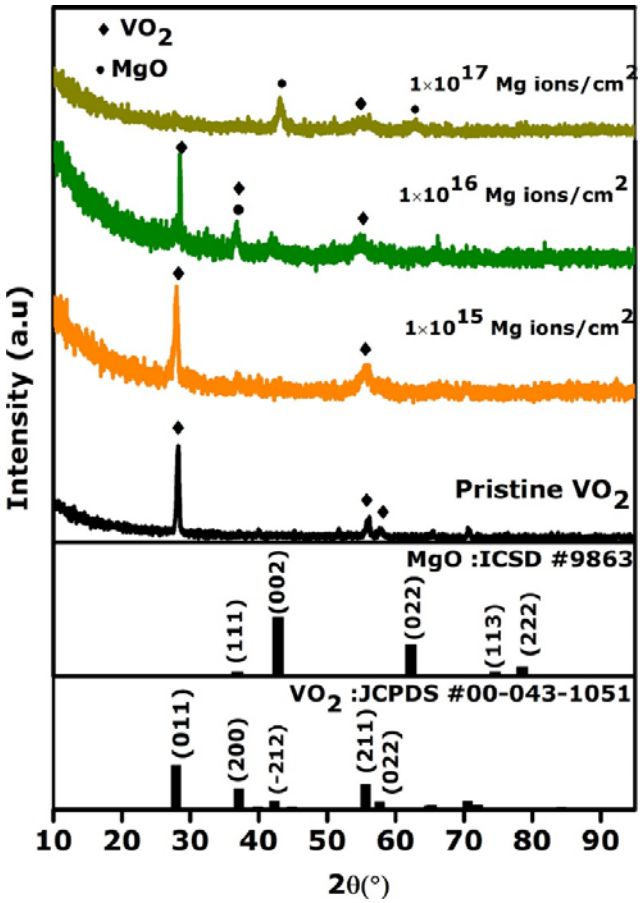

Fig. 3. XRD pattern of VO_2 thin films upon increasing Mg content from 0 to 1×10^{17} ions/cm^2 in comparison with the reference difractograns for VO_2(M1) and cubic MgO phases according to JCPDS #00-043-1051 and MgO #9863, respectively.

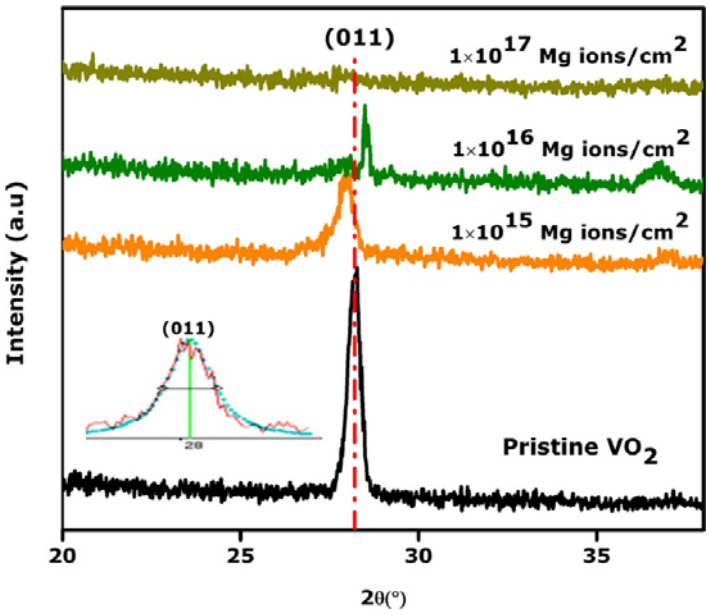

Fig. 4. XRD spectrum for the comparison of the preferential (011) orientation of pristine VO_2 sample and 35 KeV Mg ions implanted films with different fluences 1×10^{15} ions/cm^2, 1×10^{16} ions/cm^2 and 1×10^{17} ions/cm^2. It is embedded with the Debye Scherer approximation and fit of the dominant (011) peak.

Intercalation of Mg ions in the lattice lead to changes of the crystal lattice changes and the shift of the (011) peak to lower diffraction angle at the lowers fluence suggests that the crystal lattice expand. Studies conducted by Zhou et al. and Panagopoulou et al. also reveal peak shift of the (011) orientation for all doses with the creation of oxygen vacancies due to the Mg^{2+} [39,40]. Furthermore; VO_2 thin films irradiated with ions around 1 MeV revealed a shift of the (011) peak to smaller angles in all doses/fluence [33]. This was attributed to the atomic displacement in the lattice structure of VO_2 and strain in the out-of-plane direction due to high energy irradiation that creates defects. **(ii)** In contrast; the (011) peak doesn't maintain its shift towards lowers angles at 1×10^{16} ions/cm^2, it is restored towards higher diffraction angles with broadening and intensity decrease. This is due to the spontaneous irregular formation; stress and disordered layers formed by the Mg ion implantation on the VO_2 matrix. The observed trend is also attributed to the compression of the crystal lattice as the fluence increases. Nuclear collisions characterized by the implant energy, and electron stopping leads to strain/stress and relaxation development due to the clustering of interstitial defects. **(iii)** Noticeably, increasing the Mg ion fluence from 1×10^{16} to 1×10^{17} ions/cm^2 lead to the disappearance of the (011) preferential phase of VO_2 and consequently degradation of the VO_2 films. Amorphization and degradation of the VO_2 films from the irradiation effect were observed for all ion doses in high-energy W ion implantation of VO_2 thin film [41]. Metal oxides subjected to irradiations have been reported to undergo complex structural modifications (defects production, disordering, amorphization) which depend on the nature of the material, the radiation energy and the dose [33]. For the film with 1×10^{16} Mg content, the spectra show the formation of new peak at 2θ ~36° which might be attributed to (200) or (111) for VO_2(M1) or cubic MgO planes, respectively. For the highest fluence, a highly intense (002) diffraction peak is observed and it corresponded to MgO: ICSD # 9863. Similar effects were reported in Mg doping of zinc oxide films [42]

To further study the structural composition and evolution of pristine and Mg-implanted VO_2 films, RBS measurements and analysis were performed. The spectra (fitted using the

SIMNRA software) showed the vanadium edge peak (layer) mainly composed of elements appearing from the thin films (V: O: Mg), and the other peak showing the existence of Si appearing from the substrate. The intensity of the peaks from the simulated spectrum represent the percentage weight composition of the elements present in the thin films. The observed increase of the RBS spectrum yield to channel at channel ~400 attributed to Mg atoms for which the Mg concentration reaches several atomic percentages for the highest fluence used while both height and shape of the spectra change with increasing ion dose. Fig. 5 (b)–(d) clearly corroborates and demonstrates the effect of Mg ions relative to fluence on the structural composition of VO_2 thin films. Mg signatures are clearly defined in implanted films, with the distinctive observation of its intensity increases at high ion fluence and consequently decreasing the vanadium edge layer. This is supported by a clearly defined secondary orientation of the MgO signature at higher fluence as observed from XRD results in Fig. 3. As vanadium is known to exist in different valence states and consequently have many possible oxides, the ratio of the vanadium-oxygen depth profiling is relatively important for defined structural properties of vanadium oxide thin films [43]. Also, the dynamic-TRIM reveal that there is a pileup of Mg near the surface with increase of fluence which might be attributed to the insufficient ion energy leading to the shallow penetration depth. The Mg depth profile together with the enhanced concentration near the surface suggests ion-beam-induced erosion of the surface which lead to sputtering of target atoms from near surface region. These correlates with the decrease of vanadium peak intensity in Fig. 5(d) and the slight reduction of Oxygen peaks resulting in the distorted stoichiometry at relatively high fluence which compromises the film's properties.

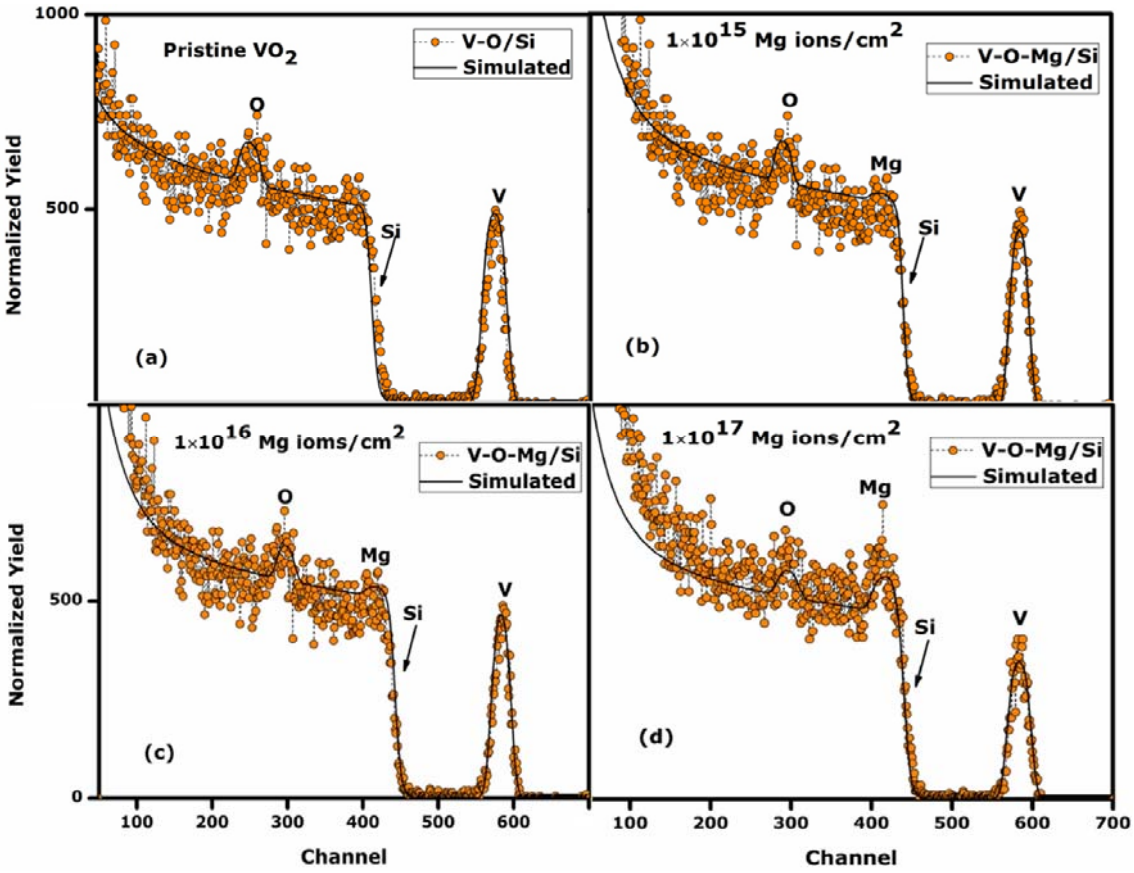

Fig. 5. RBS data with SIMNRA simulated spectra for pristine VO_2 **(a)**, and VO_2: Mg-doped thin films **(b-d)**.

3.2. Electrical properties of VO_2: Mg

Room temperature Hall effect measurements were carried out to monitor carrier concentration, Hall mobility as a function of Mg fluence. The results are illustrated in Fig. 6. Positive hall coefficients were obtained in all the samples which suggested holes as the major charge carrier of the sample. VO_2 films were deposited onto Si (100) substrate which provides additional current conduction path and care is required when interpreting hall results in this case. Pristine VO_2 showed carrier concentration and carrier mobility to be $3.54 \times 10^{19}/cm^3$ and 197 $cm^2\ V^{-1}\ S^{-1}$. Increasing Mg content tend to increase the carrier concentration from $3.54 \times 10^{19}/cm^3$ to $1.16 \times 10^{21}/cm^3$ while decreasing the carrier mobility from 197 $cm^2V^{-1}S^{-1}$ to 0.416 $cm^2V^{-1}S^{-1}$. The carrier mobility of implanted films suggests an increase in the work function (W_f) parameter. The work function of metal oxides and semiconductors increases with their average state of inhomogeneous defects and deformation accumulated [44, 45].

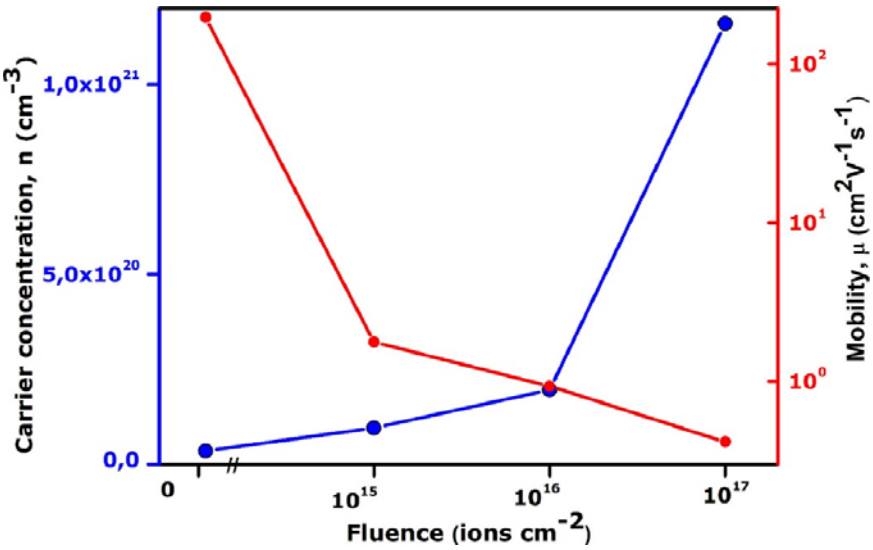

Fig. 6. Variation of carrier concentration (Blue) and carrier mobility (red) of pure and Mg implanted VO_2 samples with respect to fluence.

Phase transition characteristics of the VO_2 films were evaluated by measuring temperature-dependent resistivity at temperature ranging from 270K to 380K for the cooling and heating processes as illustrated in Fig. 7. Pure VO_2 sample exhibits a sharp decrease in film resistivity with increasing temperature and this strongly suggests the occurrence on SMT phase transition. Noticeably, the phase transition temperature (T_{tr}) of the pristine VO_2 film is well beyond the characteristic value of 68 °C and was obtained to be ~77 °C. Kana Kana et al and Madiba et al. reported on the sputtered VO_2 thin films with T_{tr} > 70 °C [46, 47]. The observed thermo-electrical transition is due to the competing effects of grain size, nucleation defects, grain boundaries, and stress crystal imperfections attributed to higher deposition temperature and film-substrate mismatch [47,48]. Observed GIXRD peak of the pristine film at 28.23° film is coherent to the film deposition stress induced on the VO_2 grains characterized by specific processes of structure evolution. Implanted VO_2 films show that the radiation-induced spatial distributions significantly affect the thermochromism, shape and magnitude of the SMT of VO_2. Increasing Mg fluence drastically decreased T_{tr} to ~ 43.49 °C and 47.74 °C for 1×10^{15} ions/cm^2 and 1×10^{16} ions/cm^2, respectively. The observed results clearly indicate that introducing the Mg ion, relative to its fluence on the structural configuration of

VO_2 lowers the phase transition of VO_2 thin film as well as affecting the overall contrast of film's resistivity wherein, the increase of Mg content in the films altered the magnitude of the transition from ~3.5 to ~1.5 orders of magnitude. These studies also showed that the induced defects alter the SMT of VO_2 by lowering both the phase transition temperature and the low-temperature-phase resistivity while the high-temperature-phase resistivity fluctuates as the dopant dose increase. The observed linear temperature-dependent resistivity configuration at 1×10^{17} ions/cm^2 consequently shows that high dose implant affect the abrupt nature of VO_2 SMT by stabilizing the low-temperature-phase as the temperature increases. It is clearly confirmed, as well from the SRIM observation that the Mg implantation spontaneously forms metal nano-particles embedded in the VO_2 matrix proportional to the implant fluence. This can be attributed to the poor crystallization of (011) preferential phase of the monoclinic VO_2 films, reduced vanadium edge layer and loss of Oxygen, confirmed in the XRD and RBS measurements.

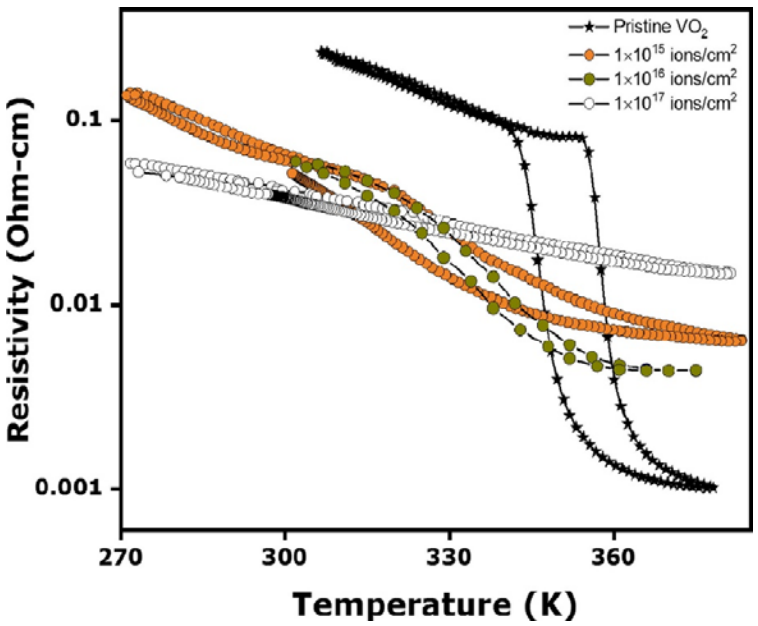

Fig. 7. Temperature-dependent sheet resistance of as-deposited, 1×10^{15} Mg ions/cm^2, 1×10^{16} Mg ions/cm^2 and 1×10^{17} ions/cm^2 thin films.

4. Conclusion

This work is based on the investigation of the effect of implanted Mg ions on the structure and electrical properties of VO_2 thin films. VO_2 thin films with a prevalent monoclinic crystal phase were successfully deposited by PLD and the desired Mg ions were successfully implanted at three different fluences 1×10^{15}, 1×10^{16} and 1×10^{17} ions/cm^2 with no foreign atom detected. The experimental data measured structurally and electrically revealed the following important results; at lower doses of Mg, the VO_2 matrix is inhomogeneously strained along the projected distribution due to radiation-induced defects. Moreover; above the 1×10^{17} ions/cm^2 fluence, Mg ions become finite on the surface of VO_2 thin films and consequently alters the SMT and surface properties of VO_2 thin film. Suggesting that with increasing fluence of Mg, loss of thermochromism is prevalent. Absence on the (011) orientation at high fluence confirms that ion implantation modifies and degrade the surface properties of VO_2 thin films. At particular higher fluences respective to the doping energy,

ion implantation compared to reported chemical doping methods degrades the characteristic SMT properties of VO_2. Thermochromism analysis revealed a drastic reduction of the semiconductor to metal phase transition temperature due to the increased Mg fluence in VO_2 films while the contrast and the width are compromised.

Declaration of Competing Interest

The authors declare that they have no known competing financial interests or personal relationships that could have appeared to influence the work reported in this paper.

Acknowledgment

The author wishes to appreciate the financial support from the National Research Foundation of South Africa. Also, to thank the GNS-Science at New Zealand, University of South Africa, University of The Western Cape, University of Pretoria and iThemba LABS (material research department) for providing the facilities required for the ion implantation and characterization facilities to analyse our samples.

References

[1] N. Muslim, Y.W. Soon, C.M. Lim, N.Y. Voo, Developments of thermochromic VO2-based thin films for architectural glazing, *IOP Conf. Ser. Mater. Sci. Eng*. 409 (1) (2018) 012016.

[2] I.G. Madida, A. Simo, B. Sone, A. Maity, J.B. Kana Kana, A. Gibaud, G. Merad,F.T. Thema, M. Maaza, Submicronic VO2–PVP composites coatings for smart windows applications and solar heat management, *Sol. Energy* 107 (2014) 758–769.

[3] F. Morin, Oxides which show a metal-to-insulator transition at the Neel temperature, Phys. Rev. Lett. 3 (1) (1959) 34–36.

[4] N.F Mott, Physics and chemistry of electrons and ions in condensed matter, in: J.V. Acrivos, N.F. Mott, A.D. Yoffe (Eds.), *Metal-Insulator Transitions,* 130 ed, Springer, Dordrecht, 1984, p. 287c29.

[5] M. Soltani, A.B. Kaye, Properties and applications of thermochromic vanadium dioxide smart coatings, *Intell. Coat. Corros. Control* (2015) 461–490.

[6] I.G Madiba, A Simo, B Sone, L Kotsedi, M Maaza, Thermochromic properties of VO2-PVP composite coatings, *Mater. Today –Proc*., 2 (7) 4006–4018.

[7] L.Zhao, L. Miao, C. Liu, C. Li, T. Asaka, Y. Kang, Y. Iwamoto, S. Tanemura, H. Gu, H. Su, Solution-processed VO2-SiO2 composite films with simultaneously enhanced luminous transmittance, solar modulation ability, and anti-oxidation property, *Sci.Rep*. 4 (2014) 7000.

[8] M. Maaza, D. Hamidi, A. Simo, T. Kerdja, A.K. Chaudhary, J.B. Kana Kana, Optical limiting in pulsed laser deposited VO2 nanostructures, *Opt. Commun*. 258 (6) (2012) 1190–1193.

[9] M. Maaza, S. Simo, B.D. Itani, J.B. Kana Kana, E.L. Harti, K. Boziane, M.L. Saboungi, T.B. Doyle, L. Lukyanchuk, J. Nanopart, Phase transition in a single VO2 nano-potential femtosecond tunable opto-electronic nano-gating, *J. Nanoparticle Res.* 16 (2014) 2397–2401.

[10] B.N. Masina, S. Lafane, L. Wu, A.A. Akande, B. Mwakikunga, S. Abdelli-Messaci, T. Kerdja, A. Forbes, Phase-selective vanadium dioxide (VO2) nanostructured thin films by pulsed laser deposition, *J. Appl. Phys.* 118 (2015) 165308.

[11] M.H. Lee, M.G. Kim, H.K. Song, Thermochromism of rapid thermal annealed VO2 and Sn-doped VO2 thin films, *Thin Solid Films* 290-291 (1996) 30–33.

[12] P. Jin, S. Nakao, S. Tanemura, "Tungsten doping into vanadium dioxide thermo-chromic films by high-energy ion implantation and thermal annealing, *Thin Solid Films* 324 (1998) 151–158.

[13] A. Paone, R. Sanjines, P. Jeanneret, H.J. Whitlow, E. Guibert, G. Guibert, F. Bussy, J.L. Scartezzini, A. Schüler, Influence of doping in thermochromic V1-x WxO2 and V1-xAlxO2 thin films: twice improved doping efficiency in V1-x WxO2. *J. Alloys Compd*. 621 (2015) 206–211.

[14] L. Song, Y. Zhang, W. Huang, Q. Shi, D. Li, Y. Zhang, Y. Xu, Preparation and thermochromic properties of Ce-doped VO2 films, Mater. Res. Bull. 48 (2013) 2268–2271.
[15] P. Kiri, M.E.A. Warwick, I. Ridley, R. Binions, Fluorine doped vanadium dioxide thin films for smart windows, *Thin Solid Films* 520 (2011) 1363–1366.

[16] T.J. Hanlon, J.A. Coath, M.A. Richardson, Molybdenum-doped vanadium dioxide coatings on glass produced by the aqueous sol-gel method, *Thin Solid Films* 436 (2003) 269–272.

[17] B.G. Chae, H.T. Kim, S.J. Yun, Characteristics of W- and Ti-doped Vo2 thin films prepared by sol-gel method, *Electrochem. Solid State* 11 (6) (2008) D53–DD5.

[18] X. Wu, Z. Wu, H. Zhang, R. Niu, Q. He, C. Ji, J. Wang, Y. Jiang, Enhancement of VO2 thermochromic properties by Si doping, *Surf. Coat. Technol*. 276 (2015) 248–253.

[19] H. Kakiuchida, P. Jin, M. Tazawa, Optical characterization of vanadium–titanium oxide films, *Thin Solid Films* 516 (2008) 4563–4567.

[20] W. Burkhardt, T. Christmann, S. Franke, W. Kriegseis, D. Meister, B.K. Meyer, W. Niessner, D. Schalch, A. Scharmann, Tungsten and fluorine co-doping of VO2 films, *Thin Solid Films* 402 (2002) 226–231.

[21] M.A. Sobhan, R.T. Kivaisi, B. Stjerna, C.G. Granqvist, Thermochromism of sputter-deposited WxV1−x O2 films, *Sol. Energy Mater Sol Cells* 44 (1996) 451–455.

[22] A. Paone, R. Sanjines, P. Jeanneret, A. Schüler, Temperature-dependent multiangle FTIR NIR–MIR ellipsometry of thermochromic VO2 and V1−x WxO2 films, *Sol Energy* 118 (2015) 107–116.

[23] T.D. Manning, I.P. Parkin, M.E. Pemble, D. Sheel, D. Vernardou, Intelligent window coatings: atmospheric pressure chemical vapor deposition of tungsten-doped vanadium dioxide, *Chem. Mat.* 16 (2012) 744–749.

[24] C.J. Patridge, L. Whittaker, B. Ravel, S. Banerjee, Elucidating the influence of local structure perturbations on the metal-insulator transitions of V12xMoxO2 nanowires: Mechanistic insights from an X-ray absorption spectroscopy study, *J. Phys. Chem. C* 116 (2012) 3728–3736.

[25] C. Batista, J. Carneiro, R.M. Ribeiro, V. Teixeira, Reactive pulsed-DC sputtered Nb-doped VO2 coatings for smart thermochromic windows, *Nanosci. Nanotechnol*. 11 (2011) 9042–9045.

[26] N. Wang, Q.S. Goh, P.L. Lee, S. Magdassi, Y. Long, One-step hydrothermal synthesis of rare earth/W-codoped VO2 nanoparticles: reduced phase transition temperature and improved thermochromic properties, *J. Alloys Compd*. 711 (2017) 222–228 31.

[27] J. Zhou, Y. Gao, X. Liu, Z. Chen, L. Dai, C. Cao, H. Luo, M. Kanahira, C. Sun, L. Yan., Mg-doped VO2 nanoparticles: hydrothermal synthesis, enhanced visible transmittance and decreased metal-insulator transition temperature, *Phys. Chem. Chem. Phys*. 15 (20) (2013) 7505–7511.

[28] S. Ji, F. Zhang, P. Jin, Preparation of high performance pure single phase VO2 nanopowder by hydrothermally reducing the V2O5 gel, *Sol. Energy Mater. Sol*. Cells 95 (2011) 3520–3526 32.

[29] Y. Zhou, S. Ji, Y. Li, Y. Gao, H. Luo, Jin, Microemulsion-based synthesis of V 1−x W x O 2 SiO2 core–shell structures for smart window applications*, J. Mater. Chem. C* 2 (2014) 3812–3819.

[30] M. Panagopoulou, E. Gagaoudakis, N. Boukos, E. Aperathitis, G. Kiriakidis, D. Tsoukalas, Y.S. Raptisa, Thermochromic performance of Mg-doped VO2 thin films on functional substrates for glazing applications, *Sol. Energy Mater. Sol. Cell* 157 (2016) 1004–1010.

[31] I. Sakaguchi, H. Ryoken, T. Nakagawa, Y. Sato, H. Haneda, Luminescence properties of Cu-ion-implanted and annealed ZnO thin films deposited by chemical vapor deposition and pulsed laser deposition, *Surf. Interface Anal*. 38 (1) (2006) 1–5.

[32] S. Kohiki, M. Nishitani, T. Wada, T. Hirao, Enhanced conductivity of zinc oxide thin films by ion implantation of hydrogen atoms, *Appl. Phys. Lett*. 64 (21) (1994) 2876–2878.

[33] I.G.Madiba, M.Chaker N.Émond, F.T. Thema, S.I. Tadadjeu, U. Muller, P.A. Braun, L. Kotsedi, M. Maaza, Effects of gamma irradiations on reactive pulsed laser deposited vanadium dioxide thin films, *Appl. Surf. Sci*. 411 (2017) 271–278.

[34] M. Panagopoulou, E. Gagaoudakis, N. Boukos, E. Aperathitis, G. Kiriakidis, D. Tsoukalas, Y.S. Raptis, Thermochromic performance of Mg-doped VO2 thin films on functional substrates for glazing applications, *Sol. Energy Mater. Sol. C* 157 (2016) 1004–1010.

[35] A. Markwitz, J. Kennedy, Group-IV and V ion implantation into nanomaterials and elemental analysis on the nanometre scale, *Int. J. Nanotechnol*. 6 (3–4) (2009) 369–383.

[36] J.P. Biersack, Computer simulations of sputtering, *Nucl. Instrum. Methods Phys. Res. Sect. B: Beam Interact. Mater. Atoms* 27 (1) (1987) 21–36.

[37] K.E. Holbert, *Radiation Effects on Materials: Displacement Damage Lectures from Nuclear Concepts for the 21st Century Course*, Arizona State University, 2006.

[38] A.G. Holmes-Siedle, L. Adams, *Handbook of Radiation Effects*, Oxford University Press, Oxford, New York, 1993.

[39] J.D. Zhou, Y.F. Gao, X.L. Liu, et al., Mg-doped VO2 nanoparticles: hydrothermal synthesis, enhanced visible transmittance and decreased metal-insulator transition temperature, *Phys. Chem. Chem. Phys*. 15 (1) (2013) 7505.

[40] Ji. Chunhui, Wu. Zhiming, Lu. Lulu, Wu. Xuefei, Wang. Jun, Liu. Xianchao, Zhou. Hongxi, Huang. Zehua, Gou. Jun, Jiang. Yadong, High thermochromic performance of Fe/Mg co-doped VO2 thin films for smart window applications, *J. Mater. Chem.* C 6 (24) (2018) 6502–6509.

[41] P. Jin, S. Nakao, S. Tanemura, High-energy W ion implantation into VO2 thin film, *Nucl. Instrum. Method B* 141 (1-4) (1998) 419–424.

[42] P. Kumar, H.K. Malik, A. Ghosh, R. Thangavel, K. Asokan, Bandgap tuning in highly c-axis oriented Zn1−xMgxO thin films, *Appl. Phys. Lett.* 102 (22) (2013) 221903.

[43] C.H. Griffith, H.K. Eastwood, Influence of stoichiometry on the metal-semi-conductor transition in vanadium dioxide, *J. Appl. Phys*. 45 (1974) 2201.

[44] M.T. Greiner, L. Chai, M.G. Helander, W.M. Tang, Z.H. Lu, Transition metal oxide work functions: the influence of cation oxidation state and oxygen vacancies, *Adv. Funct. Mater.* 22 (2012) 4557–4568.

[45] I.G Madiba, N. Émond, M. Chaker, B.S Khanyile, S.I Tadadjeu, P. Zolliker, M. Izerrouken, N. Matinise, A. Braun, M Nkosi, M Maaza, *Nucl. Instrum. Method B* 443 (2019) 25–30.

[46] J.B. Kana Kana, J.M. Ndjaka, B.D. Ngom, A.Y Fasasi, O. Nemraoui, R. Nemutudi, D. Koesen, M. Maaza, High substrate temperature-induced anomalous phase transition temperature shift in sputtered VO2 thin films, *Opt. Mater*. 32 (2012) 739–742.

[47] I.G. Madiba, L. Kotsedi, B.D. Ngom, B.S. Khanyile, M. Maaza, Effect of substrate temperature on thermochromic vanadium dioxide thin films sputtered from vanadium target, *AIP Conference Proceedings*, 1962 2018040002.

[48] B.D. Ngom, M. Chaker, A. Diallo, I.G. Madiba, S. Khamlich, N. Manyala, O. Nemraoui, R. Madjoe, A.C. Beye, M. Maaza, Competitive growth texture of Pulsed laser deposited vanadium dioxide nanostructures on a glass substrate, *Acta Mater*. 64 (2014) 32–41.